

of *Turbulent Boundary Layers—1968 AFOSR—IFP—Stanford Conference*, Vol. 1, Stanford Univ., Stanford, CA, pp. 375–383.

⁶Cooper, G. K., "The PARC Code: Theory and Usage," Arnold Engineering and Development Center, TR-87-24, Oct. 1987.

⁷Lee, J., Sloan, M. L., and Paynter, G. C., "A Lag Model for Turbulent Boundary Layers Developing over Rough Bleed Surfaces," AIAA Paper 93-2988, July 1993.

⁸Paynter, G. C., Treiber, D. A., and Kneeling, W. D., "Modeling Supersonic Inlet Boundary Layer Bleed Roughness," *Journal of Propulsion and Power*, Vol. 9, No. 4, 1993, pp. 622–627.

⁹Spalart, P. R., and Allmaras, S. R., "A One-Equation Turbulence Model for Aerodynamic Flows," AIAA Paper 92-0439, Jan. 1992.

¹⁰Betterman, D., "Contribution à l'Etude de la Couche Limite Turbulente le Long de la Plaques Rugueuses," Centre National de la Recherche Scientifique, Rept. 65-6, Paris, 1965.

¹¹Arndt, R. E. A., and Ippen, A. T., "Cavitation near Surfaces of Distributed Roughness," Hydrodynamics Lab., Dept. of Civil Engineering, Massachusetts Inst. of Technology, Rept. 104, Cambridge, MA, 1967.

¹²Coleman, H. W., Moffat, R. J., and Kays, W. M., "Momentum and Energy Transport in the Accelerated Fully Rough Turbulent Boundary Layer," Dept. of Mechanical Engineering, Stanford Univ., Rept. HMT-24, Stanford, CA, 1976.

¹³Scott, V. E., and Power, J. L., "The Influence of Pressure Gradient on the Turbulent Boundary Layer over a Rough Surface," Navy Dept., David Taylor Model Basin, Washington, DC, Rept. 2115, 1965.

Boundary-Layer Tripping by a Roughness Element

Jamal A. Masad*
High Technology Corporation,
Hampton, Virginia 23666

Introduction

BOUNDARY-LAYER tripping is desired in scramjet as well as heat-exchanger design to enhance, respectively, mixing and heat transfer rates. Furthermore, the achievement of earlier transition by artificial tripping of the boundary layer is often desired in wind-tunnel operations to simulate turbulent boundary-layer behavior at full-scale Reynolds numbers. The most common method for tripping the boundary layer is the use of roughness. The existence of roughness enhances the instability of the flow and accelerates the onset of transition and, consequently, the occurrence of turbulence. It is known that tripping the boundary layer with roughness elements becomes more difficult at higher speeds. This was first evident because large-diameter wires were needed to trip the boundary layer at high speeds.

The occurrence of laminar separation on aerodynamic surfaces increases pressure drag that results in a reduction in the efficiency of these surfaces. Separation can result from a localized adverse pressure gradient created by surface roughness, or it can result from extended regions of adverse pressure gradient because of the curvature of the surface. In both cases, the flow may separate while it is still laminar.¹ In situations in which laminar separation is about to occur, tripping the boundary layer so that it remains attached is preferable. Transition causes the point of separation to move downstream because in

a turbulent boundary layer the accelerating influence of the external flow extends farther because of turbulent mixing. This in turn, reduces the pressure drag.

The critical tripping height of a roughness element is defined as the minimum height that causes transition at the downstream end of the roughness element. In this work, we quantify the variation of the critical tripping height of a roughness element with parameters such as the freestream Mach and Reynolds numbers and the length of the roughness element. Our approach consists of using linear stability theory, coupled with the empirical e^N method, to predict the transition onset location.

The presence of a roughness element on a surface can produce a separation bubble behind it if and when its height becomes sufficiently large. In such flows, both a strong viscous-inviscid interaction and an upstream influence are known to exist. The conventional boundary-layer formulation fails to predict such flows; therefore, one needs to use a triple-deck theory, an interacting boundary layer (IBL) theory,² or a Navier–Stokes solver to analyze them. In this work we use the IBL theory to predict such flows.

The numerical results presented in this work are for two-dimensional compressible subsonic flow over a single, smooth, two-dimensional hump on a flat plate. The results are for a two-parameter family of symmetric hump shapes given by

$$y = y^*/L^* = (k^*/L^*)f(z) = kf(z) \quad (1)$$

where

$$z = 2(x^* - L^*)/\lambda^* = 2(x - 1)/\lambda \quad (2)$$

$$f(z) = \begin{cases} 1 - 3z^2 + 2|z|^3, & \text{if } |z| \leq 1 \\ 0, & \text{if } |z| > 1 \end{cases} \quad (3)$$

Here, k^* is the dimensional height of the symmetric hump; it is positive for a hump and negative for a dip. The parameter λ^* is the dimensional length of the hump with the center located at $x^* = L^*$.

For stability analysis, we use spatial quasiparallel instability. By solving the linear instability eigenvalue problem, we obtain the disturbance-wave growth rate as a function of location on the flat surface. The transition onset location is then empirically correlated with the location at which the integrated growth rate (N factor) of the disturbance wave reaches a certain value. This is the empirical N -factor transition criterion (i.e., the criterion that utilizes the e^N method) proposed by Smith and Gamberoni³ based on experimental data (see also Jaffe et al.⁴). For flow over a flat plate, transition was found to occur when the N factor reached a value close to 9. We denote the value of Re_x at which the N factor reaches a value of 9 by $(Re_x)_{N=9}$.

The length of a roughness element influences considerably the predicted transition onset location.⁵ However, the effect of the length of a roughness element on flow instability and transition location is usually overlooked in the literature. Although the experimental correlations of Fage⁶ and Carmichael⁷ account for the effect of roughness length on transition location, the commonly used Re_k correlation does not.

The role of the hump length is opposite that of the hump height. If the nondimensional length $\lambda = \lambda^*/L^*$ of a hump at a fixed height is decreased, then the location where the N factor first reaches a value of 9 is shifted upstream. When the roughness element becomes so short that its length falls below a certain critical value, the upstream movement of the transition location slows down considerably, and the predicted transition location approaches the downstream end of the roughness element.

Variation of the nondimensional critical tripping height k_{crit} with the nondimensional length of the hump λ is shown in Fig. 1. The results are for incompressible flow at a freestream

Received Sept. 23, 1995; revision received Feb. 14, 1996; accepted for publication Feb. 22, 1996. Copyright © 1996 by the American Institute of Aeronautics and Astronautics, Inc. All rights reserved.

*Research Scientist, 28 Research Drive, P.O. Box 7262. Senior Member AIAA.

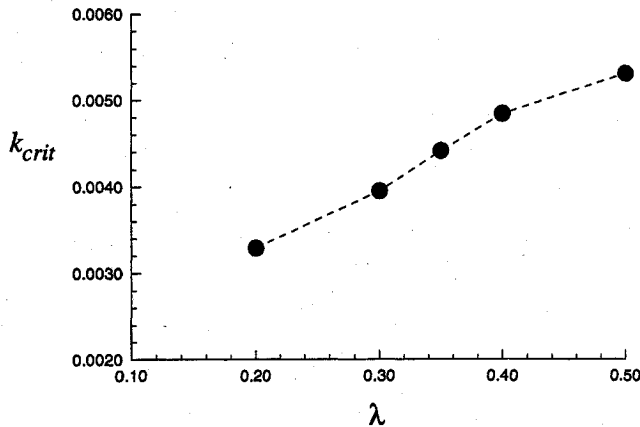


Fig. 1 Variation of the critical tripping height of a hump with hump's length.

Reynolds number of $Re = 10^6$. It is clear from Fig. 1 that increasing the length of the hump increases its critical tripping height. However, the variation is not linear and it seems that the rate of increase of k_{crit} becomes smaller for relatively long humps.

The effect of compressibility on the stability characteristics of two-dimensional flow over roughness elements is complicated by the fact that although an increasing Mach number stabilizes the flow in the attached regions, it increases the size of the separation bubble.⁵ An increase in the value of the free-stream Mach number M_∞ causes the flow over the hump to separate at lower hump heights because compressibility makes the pressure gradient more adverse and enhances separation. When the flow separates, increasing the freestream Mach number increases the length of the separation bubble by shifting the separation location slightly upstream and shifting the reattachment location considerably downstream. In their experimental work, Larson and Keating⁸ noticed a large increase in the streamwise length of the separation region when the Mach number of the flow over the roughness element was increased.

The widening of the separation region because of the increase in M_∞ partially offsets the stabilizing effect of compressibility. Overall, in two-dimensional flow, the stabilizing effect of compressibility in the attached regions overcomes the destabilization caused by the increase in the size of the separation bubble. The downstream movement of the transition location of a flow over a step as the Mach number increases was noticed and reported by Chapman et al.⁹ Van Driest and Boisson¹⁰ studied experimentally the effect of two-dimensional surface roughness (circular wire) mounted on a cone on transition at supersonic Mach numbers. They indicated a spectacular role of Mach number in damping the effect of roughness on transition. They also indicated that with increasing Mach numbers, increasingly large ratios of roughness height to boundary-layer displacement thickness were necessary to promote transition. Furthermore, the stability of a laminar shear layer (that develops in the case of separation) was found by Lin¹¹ to increase markedly as the Mach number increases. At supersonic speeds in wind-tunnel operation, larger wire diameters are required to trip the boundary layer as the Mach number increases (see, e.g., Coles¹²).

In Fig. 2 we present computational results that support and agree with all of the previously indicated experimental observations. The results are for a hump of length $\lambda = 0.2$ and the freestream Reynolds number is $Re = 10^6$. It is clear that the critical tripping height of the hump increases with freestream Mach number in the considered subsonic range. Furthermore, Fig. 3 shows a consistent increase in the rate of change of k_{crit} with M_∞ as M_∞ increases. While the critical tripping height for incompressible flow is $k_{crit} = 0.0033$, the corresponding value for $M_\infty = 0.7$ flow is $k_{crit} = 0.0045$.

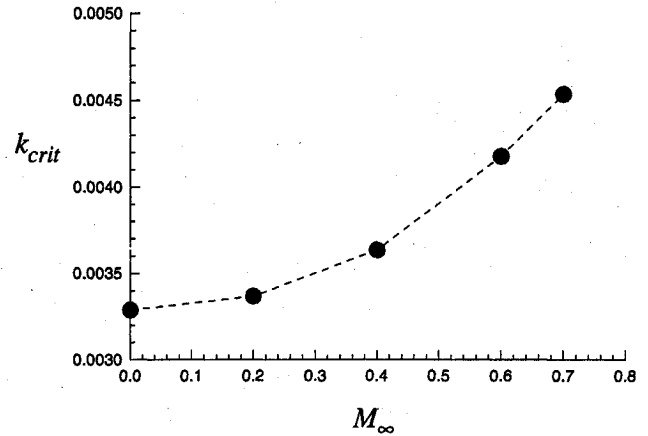


Fig. 2 Variation of the critical tripping height of a hump with freestream Mach number.

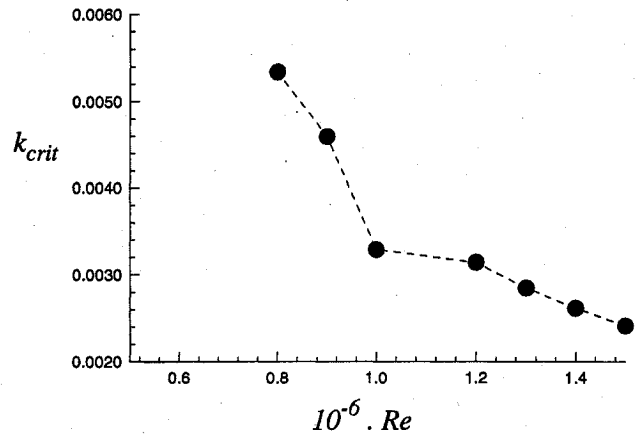


Fig. 3 Variation of the critical tripping height of a hump with freestream Reynolds number.

As the freestream Reynolds number of flow over a roughness element increases, the predicted transition onset location moves to upstream locations.⁵ Moreover, increasing the freestream Reynolds number enhances boundary-layer separation. Fage and Preston¹³ performed a wind-tunnel experimental study for flow past a wire mounted on a body of revolution. They noticed that at a certain freestream velocity the flow formed separation vortices, but the flow was laminar far downstream of the wire. Increasing the freestream velocity (which increases the freestream Reynolds number), moved the transition point closer to the wire.

The results in Fig. 3 support and agree with experimental observations such as the previously indicated observation of Fage and Preston. The results that are for incompressible flow with $\lambda = 0.2$ show clearly that increasing the freestream Reynolds number reduces the critical tripping height.

In summary, the critical tripping height of a roughness element is defined as the minimum height at which transition occurs at the downstream end of the roughness element. The variation of the critical tripping height of a hump in subsonic flow over a flat surface with freestream Mach and Reynolds numbers and hump's length is quantified. It is found that increasing the freestream Mach number, decreasing the freestream Reynolds number, and increasing the length of the hump result in an increased critical tripping height of the hump.

References

- Masad, J. A., and Malik, M. R., "Link Between Flow Separation and Transition Onset," *AIAA Journal*, Vol. 33, No. 5, 1995, pp. 882-887.

²Davis, R. T., "A Procedure for Solving the Compressible Interacting Boundary Layer Equations for Subsonic and Supersonic Flows," AIAA Paper 84-1614, 1984.

³Smith, A. M. O., and Gamberoni, N., "Transition Pressure Gradient and Stability Theory," Douglas Aircraft Co. Rept. ES 25388, El Segundo, CA, 1956.

⁴Jaffe, N. A., Okamura, T. T., and Smith, A. M. O., "Determination of Spatial Amplification Factors and Their Application to Predicting Transition," *AIAA Journal*, Vol. 8, No. 2, 1970, pp. 301-308.

⁵Masad, J. A., and Iyer, V., "Transition Prediction and Control in Subsonic Flow over a Hump," *Physics of Fluids*, Vol. 6, No. 1, 1994, pp. 313-327.

⁶Fage, A., "The Smallest Size of Spanwise Surface Corrugation Which Affect Boundary Layer Transition on an Airfoil," British Aeronautical Research Council, 2120, 1943.

⁷Carmichael, B. H., "Surface Waviness Criteria for Swept and Un-swept Laminar Suction Wings," Northrop Aircraft Rept. NOR-59-438 (BLC-123), 1957.

⁸Larson, H. K., and Keating, S. J., "Transition Reynolds Numbers of Separated Flows at Supersonic Speeds," NASA TN D-349, 1960.

⁹Chapman, D. R., Kuehn, D. M., and Larson, H. K., "Investigation of Separated Flows in Supersonic and Subsonic Streams with Emphasis on the Effect of Transition," NACA Rept. 1356, 1958.

¹⁰Van Driest, E. R., and Boison, J. C., "Experiments in Boundary-Layer Transition at Supersonic Speeds," *Journal of the Aeronautical Sciences*, Vol. 24, 1957, pp. 885-899.

¹¹Lin, C. C., "The Theory of Hydrodynamic Stability," Cambridge Univ. Press, Cambridge, England, UK, 1955.

¹²Coles, D., "Measurements of Turbulent Friction on a Smooth Flat Plate in Supersonic Flows," *Journal of the Aeronautical Sciences*, Vol. 21, No. 7, 1954, pp. 433-448.

¹³Fage, A., and Preston, J. H., "On Transition from Laminar to Turbulent Flow in the Boundary Layer," *Proceedings of the Royal Society of London*, Vol. 178, 1941, pp. 201-227.

Whistler-Driven, Electron-Cyclotron-Resonance-Heated Thruster: Experimental Status

B. W. Stallard* and E. B. Hooper†

Lawrence Livermore National Laboratory,
Livermore, California 94551

and

J. L. Power‡

NASA Lewis Research Center, Cleveland, Ohio 44135

Introduction

EXPANSION of an electron-cyclotron-resonance- (ECR) heated plasma in a magnetic nozzle offers several potential advantages over other plasma thrusters for generating high specific impulse I_{sp} . The use of microwaves eliminates electrodes, a primary life-limiting component for most plasma devices; space charge ion acceleration eliminates the acceleration grid problems of ion thrusters; and wall interactions are less than other plasma thrusters, reducing energy and particle losses and the sputtering of wall material. In addition, an ECR thruster can deliver very high-power density and offers the

Received June 4, 1995; revision received Dec. 20, 1995; accepted for publication Feb. 6, 1996. Copyright © 1996 by Lawrence Livermore National Laboratory. Published by the American Institute of Aeronautics and Astronautics, Inc., with permission.

*Physicist, Magnetic Fusion Energy, Energy Directorate.

†Assistant Deputy Associate Director, Magnetic Fusion Energy, Energy Directorate. Member AIAA.

‡Aerospace Engineer, M/S 301-3. Member AIAA.

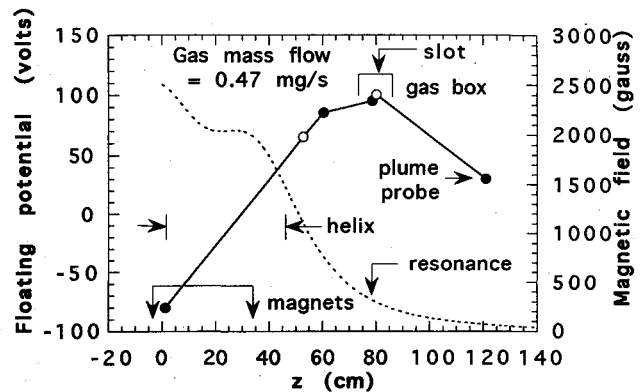


Fig. 1 Magnetic field (dashed line) and floating potentials along the plasma. Shown are potential measurements on axis (solid points) and edge (open points). Gas propellant is injected through the slot into a nine-section gas box.

possibility of variable I_{sp} through control of the plasma potential. In this Note we summarize for the propulsion community the experimental status of an approach¹⁻³ proposed to overcome limitations of previous ECR thrusters,⁴⁻⁷ especially plasma density limited by microwave cutoff at frequencies below the plasma frequency, significant power losses to atomic radiation, and plasma recycling at an interior rear wall in contact along the magnetic field.

In our experiment several new features are used. First, whistler waves are excited in the plasma at a magnetic field strength B higher than resonance given by $B_{res} = (m_e/e)2\pi f$, where f is the microwave frequency, and m_e and e are the electron mass and charge, respectively. The wave frequency satisfies $f < f_{ce}$, f_{pe} , where $f_{ce} = eB/2\pi m_e$ is the local electron cyclotron frequency (typically ~5 GHz), $f_{pe} = (1/2\pi)\sqrt{e^2 n_e / \epsilon_0 m_e}$ is the plasma frequency (typically ~6 GHz), n_e is the electron density, and ϵ_0 is the free space permittivity. The whistler wave is the only electron wave that propagates at arbitrarily high densities.⁸ Second, the resonance is located on the side of a magnetic hill below the peak field, as shown in Fig. 1. This reduces power flow up the hill to the rear boundary because the magnetic flux tube area decreases as the field increases. Third, hydrogen is injected in a gas box at a field below the resonance, where it is ionized by the heated electrons. Calculations predict that the magnetic forces caused by the anisotropic ECR electron distribution can greatly reduce energy losses up the hill.^{3,9} Fourth, the use of hydrogen or deuterium minimizes energy losses from atomic line radiation.

Floating potentials ≥ 100 V are generated in the plasma as predicted⁹ and an ion flux down the magnetic field is generated with energy characteristic of these potentials. We have also measured the excited whistler waves and their propagation and absorption in overdense plasma at the resonance. Observed discharge particle and energy efficiencies are lower than expected, probably because the injected gas is not fully ionized and losses to the rear wall are greater than predicted. Modifications to achieve high efficiencies are suggested.

Description of the Experiment

The apparatus is shown in Fig. 2. Microwaves at $f = 915$ MHz ($B_{res} = 0.0327$ T) and power up to 20 kW (30-100 ms pulse length) are coupled from a bihelical antenna to a plasma column at a magnetic field strength typically near 0.21 T. The antenna is in air, outside a 4.9-cm-i.d.-fused silica tube vacuum envelope to prevent electrical breakdown problems.³ The axial magnetic field profile, shown in Fig. 1, is generated by two solenoidal magnets located at $z = -4.3$ and 34.4 cm, with mean conductor radii of 27.9 cm.³ The magnitude, axial profile, and resonance location are varied by changing magnet currents. The resonance is between the wave-launching column and the gas box, slightly upfield of the gas box slot, as